

Nonlinear Teager-Kaiser Infomax Boost Clustering Algorithm for Brain Tumor Detection Technique

P. M. Siva Raja^{1,*}, S. Brinthakumari² and K. Ramanan³

¹Computer Science and Engineering, Amrita College of Engineering and Technology, Nagercoil, 629901, India

²Information Technology, K. C College of Engineering and Management Studies and Research, Thane, India

³Computer Science and Engineering, NPR College of Engineering and Technology, Dindigul, 629902, India

*Corresponding Author: P. M. Siva Raja. Email: selvamsivaraja@gmail.com

Received: 12 February 2022; Accepted: 29 June 2022

Abstract: Brain tumor detection and division is a difficult tedious undertaking in clinical image preparation. When it comes to the new technology that enables accurate identification of the mysterious tissues of the brain, magnetic resonance imaging (MRI) is a great tool. It is possible to alter the tumor's size and shape at any time for any number of patients by using the Brain picture. Radiologists have a difficult time sorting and classifying tumors from multiple images. Brain tumors may be accurately detected using a new approach called Nonlinear Teager-Kaiser Iterative Infomax Boost Clustering-Based Image Segmentation (NTKFIBC-IS). Teager-Kaiser filtering is used to reduce noise artifacts and improve the quality of images before they are processed. Different clinical characteristics are then retrieved and analyzed statistically to identify brain tumors. The use of a BraTS2015 database enables the proposed approach to be used for both qualitative and quantitative research. This dataset was used to do experimental evaluations on several metrics such as peak signal-to-noise ratios, illness detection accuracy, and false-positive rates as well as disease detection time as a function of a picture count. This segmentation delivers greater accuracy in detecting brain tumors with minimal time consumption and false-positive rates than current state-of-the-art approaches.

Keywords: Brain tumor detection; image segmentation; nonlinear teager kaiser filtering

1 Introduction

Tumors in the brain are generated by the growth of abnormal cells, which then spread to other parts of the brain. It may be caused by abnormal cell development in the brain. Brain tumor detection and division is a difficult tedious undertaking in clinical image preparation. When it comes to the new technology that enables accurate identification of the mysterious tissues of the brain, MRI is a great tool. It is possible to alter the tumor's size and shape at any time for any number of patients by using the brain picture. Radiologists have a difficult time sorting and classifying tumors from multiple images.



This work is licensed under a Creative Commons Attribution 4.0 International License, which permits unrestricted use, distribution, and reproduction in any medium, provided the original work is properly cited.

Reference [1] shows that Tumors are classified as either malignant or noncancerous. It has been proved that the third level of brain tumors is also malignant, which leads to death, much as the greatest degree of cancer. Early detection and treatment are critical for patients [2]. Both benign and malignant brain tumors are regarded to constitute a threat. At long last, the tumor spreads to the brain, where it may smooth out the other growth in the region. It is possible to have a primary tumor and a secondary one in the same brain. The original tumor originates in the brain tissues, whereas the secondary tumor spreads to the skull from other areas of the body [3]. Additionally, MRI is used to identify cancers since it offers information on the organization of human soft tissue that is engaged in radiography, which may help to understand the human body's structure [4]. Because of its ability to shift between different soft tissues, MRI is more important and beneficial in medical imaging. In addition, the MRI picture carries the tumor's information along with it. As one of the most effective medical imaging procedures, the MRI stands out among the many options available today.

The MRI is used extensively in advanced neuroscience research to analyze the brain's structure and function. Soft tissue structure may be shown clearly in MR pictures. Also, MR imaging has greatly improved the ability to identify and document brain disease. Computerized image analysis methods are needed because the amount of data for human interpretation is too large [5]. The MRI scan is regarded as superior to the CT scan because it has a great ability to see soft tissue [6]. MR images are more often used for the site identification and growth imaging of brain tumors because of their increased precision [7]. While CT and X-ray pictures are rigid, MR images are more flexible [8]. Because radiation is harmful to the human body, MR pictures offer the benefit of not relying on it. In addition, for MRI classification, knowledge-oriented systems, atlas approaches, shaped techniques, fuzzy schemes, variation segmentation, and neural networks are used [9]. Two well-established techniques supervised and unsupervised procedures, are used for MRI classification. The Supervised processes combine the k-nearest neighbors, the Artificial Neural Network (ANN), and the support vector machine. Fuzzy c-means plus a self-organization map make up the unsupervised technique. The supervised and unsupervised MRI classification approach has been applied in many studies [10].

The ability to withstand numerous MRI protocols and get protocol certifications for a variety of pictures [11]. MR images are utilized to identify the tumor component by injecting a different product into the tumor sector [12]. The most recent medical imaging inquiry has encountered some challenges in recognizing the brain tumor in MR pictures. Among many patients, tumor tissue may be distinguished from normal tissue, although most of the time the two are linked. The anatomical structure of the tissue may be precisely seen using MR imaging [13]. The information obtained by MR imaging is particularly helpful in the detection of a brain tumor [14]. When using a computer-assisted clinical tool to diagnose a brain tumor, the MR images must be segmented precisely. The segmentation of a brain picture is required for the detection of a brain tumor of some kind.

The task of manually segmenting MRI scans of the brain requires considerable expertise. Furthermore, for this, non-uniform segmentation, a lot of time, a non-repeatable assignment, and segmentation results are required. There are situations when a computer-assisted tool may be quite helpful in this regard [15].

An area of ongoing study in the field of computerized medical diagnosis is brain tumor segmentation, which has a high fatality rate because of brain tumors in MR images. Select findings from the calculated tomography are shown in the MRI. Also, it gives a large variance across numerous soft tissues of the human body in computerized medical diagnostic systems. As time goes on, the MRI will be much more useful for brain and cancer imaging [16]. An MRI image's characteristics are regarded as significant since they represent a picture in its smallest form. Classifiers may classify tumors as normal or malignant using additional feature extraction techniques [17]. In this case, the MRI is the preferred medical imaging technique, with the image focusing on soft tissues including tendons, ligaments, and brain tissue. With

MRI, you do not have to worry about being harmed in any way. This categorization method has been used by several researchers in the classification of medical pictures. MRI, X-ray, Computed Tomography (CT), and Positron Emission Tomography (PET) are all now used to identify tumours, but the MRI imaging approach is considered to be the best because of its enhanced decision-making capabilities. k-NN Based Classification of Brain MRI Images were introduced in [18] to categorize the benign or malignant tumor. However, the disease detection time was higher. Tumors may be identified using the MRI approach [19]. The radiologists review the MRI to identify the presence of abnormalities based on the visual clarity of the images [20]. To reduce the dimension of the 3D model was proposed the data are projected to the low-dimensional subspace to reduce the complexity of data processing using the principal component analysis (PCA) model. A two-stage reversible robust audio watermarking algorithm is proposed to protect medical audio data. The scheme decomposes the medical audio into two independent embedding domains, embeds the robust watermark and the reversible watermark into the two domains respectively.

The random discrete doping (RDD) [21] in the active device area is used to derive an analytical model to compute the standard deviation, $\sigma_{V_{th}}$, RDD of the V_{th} -distribution for any arbitrary channel doping profiles. However, improved device performance tends to offer lower V_{th} variability. Medical image processing made [22] it possible to diagnose various dangerous diseases like cancer and tumor at an early stage. But extracting the correct boundaries of the infected region through segmentation is a major challenge. Machine learning tools and optimization methods are analysis of biomedical signals that greatly benefits the healthcare sector by improving patient outcome through early, reliable detection.

2 Proposed Methodology

Medical imaging is the practice of capturing pictures of the human body's interior organs to aid in the diagnosis of disease. Using these pictures, clinicians can more easily identify the widest range of brain tumor types. As a result of the optic nerves being damaged, Brain tumor is the main cause of memory loss. Because repairing injured optic nerves is so difficult, early diagnosis of Brian tumors is particularly important. As a result, it is essential to identify automatic detection of brain's tumor. Conventionally, the identification of brain tumors using various machine learning algorithms is quite common. However, it is still inefficient in terms of addressing the issue of precise detection while using the least amount of time possible. Brain tumor identification is carried out using NTKFIBC-IS, an effective segmentation approach.

Fig. 1 depicts the suggested NTKFIBC-IS method for detecting illness properly by image segmentation, as shown. An MRI image dataset is used to count the number of MRI pictures. After the pictures are collected, the Nonlinear Teager-Kaiser filtering approach is used to reduce noise artifacts and improve image quality for precise illness detection. The Infomax boost clustering algorithm is then used to separate the picture into its component components and extract the area of interest. Afterward, the picture feature is retrieved from the inputs. As a final step, all the retrieved characteristics are compared to the illness feature that is being tested. As a consequence, the MRI pictures of brain's tumor illness have been recognized as normal. Following is a breakdown of the steps involved in implementing the NTKFIBC-IS approach as outlined above.

2.1 Nonlinear Teager-Kaiser Filtering Technique

The first step of the proposed NTKFIBC-IS technique is image preprocessing to obtain the contrast enhancement image for accurate brain tumor detection. The contrast enhancement is obtained using the Nonlinear Teager-Kaiser filtering technique.

Let us consider the input funds images ' $\delta_i = \delta_1, \delta_2, \dots, \delta_N$ ' are collected from the Image Database. Each image consists of different pixels $\delta_i = b_1, b_2, \dots, b_n$ represented in the filtering windows in the

form of rows (i) and columns (j). Then the Nonlinear Teager-Kaiser filtering highlights the edges and suppresses the noise. Then the images are warped and interpolated as given below,

$$V(i, j) = \left(\sum_{i=1}^n \sum_{j=1}^m w_a b_{ij} \right) \quad (1)$$

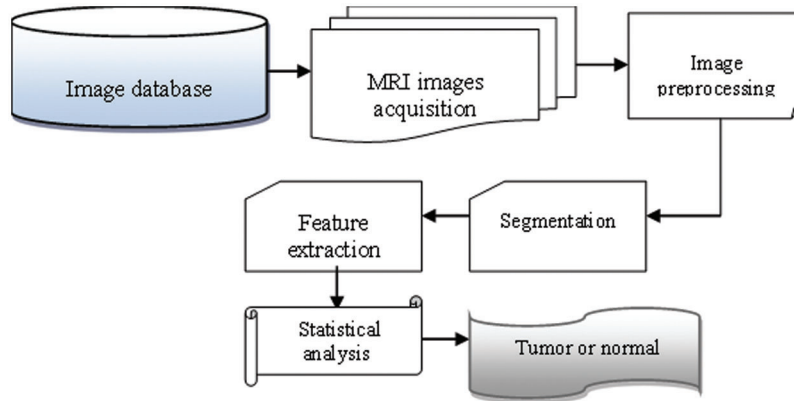


Figure 1: Flow process of the NTKFIBC-IS technique

From (1), $V(i, j)$ denotes an output of the warping and interpolation to make an image smooth, w_a be the warp matrix, b_{ij} is the pixels of the image. Image warping is used for digitally manipulating an input fundus image and correcting the image distortion. Then the normalization of input pixels is applied for ordering the range of pixel intensity values from minimum to maximum.

$$N_{ij} = \frac{V(i, j) - \min(V(i, j))}{\max(V(i, j)) - \min(V(i, j))} \quad (2)$$

From (2), N_{ij} is the normalized output of the pixels $V(i, j)$ denotes pixels from the warped and interpolation, min and max denotes a minimum and maximum value of pixels in the warping and interpolation. After the normalization, images are then applied to median denoising for smoothing the input image by removing the artifacts and obtaining the final super resolutions fundus image. The formula for denoising the input image is expressed as given below,

$$F(x) = med\{N(b_{ij})\} \quad (3)$$

In the above Eq. (3), ' $F(x)$ ' denotes an output of the median denoising and Med denotes a median, $N(b_{ij})$ denotes a normalized value of the pixels using warped and interpolation. The resulting normalized values are sorted ascending, with the median being the value in the middle. The median value of image pixels in the filtering window replaces the pixels' center values, removing the noisy ones.

2.2 Infomax Boost Clustering-Based Image Segmentation

When a group of pixels with similar features are used to separate a picture, this technique is known as image segmentation. There is a wide range of uses for this technology, from compressing images and identifying objects to identifying diseases and other diseases. To process a whole picture using this method would be very inefficient. Images may then be segmented for further processing using image segmentation. Using the Infomax boost clustering algorithm, images may be segmented for further analysis.

The infomax boost clustering is a machine learning ensemble technique that provides strong clustering results by combing the weak hypothesis. A weak hypothesis is a base clustering technique that provides slightly accurate results. On the contrary, a boost clustering technique provides well-correlated results with the true output results. Therefore, the proposed technique uses the ensemble clustering technique to improve brain's tumor detection accuracy and minimizes time consumption.

The ensemble technique uses mutual informative k means the clustering technique is a weak hypothesis. Clustering is the method of grouping similar pixels into dissimilar clusters. Initialize the 'k' number of clusters R_1, R_2, \dots, R_k and also centroid $s_1, s_2, s_3 \dots s_k$. Then the mutual dependence between the cluster centroid and the pixels in the input image is measured. Mutual dependence is the probabilistic measure that groups the pixels into different clusters. These are the probability of the two clusters being mutually dependent:

$$md(b_i, s_k) = p(b_i, s_k) \log_2 \left(\frac{p(b_i, s_k)}{p(b_i)p(s_k)} \right) \quad (4)$$

From (4), $md(b_i, s_k)$ indicates a mutual dependence between pixels (b_i) and cluster centroid s_k , $p(b_i, s_k)$ represents the joint probability distribution, $p(b_i)$ and $p(s_k)$ symbolizes a marginal probability. By using (4), the mutual dependence between the pixels and cluster centroid is computed. Then the gradient ascent function is used for finding the maximum dependence between the pixels and cluster centroid.

$$D = \arg \max md(b_i, s_k) \quad (5)$$

where, D indicates a gradient ascent function, $\arg \max$ denotes an argument of the maximum function to group similar pixels. The weak hypothesis results did not improve the clustering performance but it has some errors. So, the weak hypothesis results are boosted to obtain accurate results. The weak hypotheses are summed to obtain the final strong clustering results.

$$W = \sum_{i=1}^n g_i(b_i) \quad (6)$$

where W denotes strong clustering results, and $g_i(b_i)$ symbolizes a weak hypothesis output. After that, a similar weight is assigned with w_t to each weak cluster.

$$W = \sum_{i=1}^n g_i(b_i) * \beta \quad (7)$$

where β indicates the weight of the weak hypotheses. The weight is a random integer. Followed by, the training error is estimated based on actual and predicted errors.

$$\varphi_E = (\varphi_a - \varphi_p)^2 \quad (8)$$

In (8), φ_E indicates a training error, φ_a denotes an actual error, φ_p represents a predicted error. Based on the error, weights get updated. Incorrectly grouped patterns gain a higher weight. If the weak hypotheses are correctly grouped, then the weight is minimized. As a result, strong clustering results are obtained. Based on the clustering results, the different segments of the regions are obtained.

3 Experimental Analyses

Experimental analysis of the proposed NTKFIBC-IS technique is used in two existing systems [1] and [2]. The use of a BraTS2015 database enables the proposed approach to be used for both qualitative and quantitative research. This dataset was used to do experimental evaluations on several metrics such as peak signal-to-noise ratios, illness detection accuracy, and false-positive rates as well as disease detection

time as a function of a picture count. This segmentation delivers greater accuracy in detecting brain tumors with minimal time consumption and false-positive rates than current state-of-the-art approaches.

3.1 Dataset Description

BraTS2015

The annual undertaking of BraTS (Brain Tumor Segmentation using Multimodal Techniques) since 2012 following the MICCAI session. Different low-and high-grade gliomas in the brain are used for training in the BraTS2015, along with mixed high-and low-grade brain pictures for assessment. Skull-removed photos play a role in the proposed work. Accordingly, a few statistical parameters are given high regard by incorporating the results of segmentation into the supplied BraTS system.

3.2 Quantitative Analysis

The suggested NTKFIBC-IS methodology and the two associated techniques have been quantitatively analyzed using various quantitative metrics, such as the peak signal-to-noise ratio, illness diagnosis accuracy, false-positive rate, and detection time.

The mean square error of the difference between the original noisy picture and the quality-enhanced image is used to calculate the peak signal-to-noise ratio. The following is the formula for calculating the mean square error and the peak signal to noise ratio.

$$MSE = (\delta_i - \delta_{qe})^2 \quad (9)$$

$$PSNR = 10 * \log_{10} \left[\frac{Q^2}{MSE} \right] \quad (10)$$

where, *MSE* symbolizes a mean square error, δ_i signifies the original image and δ_{qe} be a quality enhanced image, *PSNR* represents Peak Signal to Noise Ratio, *Q* indicates a Maximum possible pixel value of the brain images (i.e., 255). The PSNR is measured in terms of decibel (dB).

Disease Detection Accuracy is defined as the ratio of several MRI images accurately detected as brain tumor or normal from the total number of MRI images.” Therefore, the accuracy of disease detection is mathematically expressed as follows,

$$DDA = \left[\frac{K_a}{N} \right] * 100 \quad (11)$$

When *N* is the total number of fundus photos, and *K_a* is the number of fundus images successfully diagnosed as brain tumor or normal, the value of *DDA* reflects the disease detection accuracy, and *N* is the total number of fundus images. Accuracy in illness detection is assessed in percentages (percent).

Time spent by an algorithm to identify a picture as normal or glaucoma may be used to measure illness detection time. Therefore, the overall disease detection time is expressed as follows,

$$DDT = N * t(DDS) \quad (12)$$

where, *DDT* disease detection time, ‘*N*’ indicate several fundus images, ‘*t(DDS)*’ specifies the time taken by the algorithm to process and detect the single fundus image. The disease detection time is measured in milliseconds (ms).

Table 1 shows the peak signal-to-noise ratio performance analysis with different picture sizes derived from the ARIMA database. The 10 distinct peak signals to noise ratios for each approach are shown in the table value.

Table 1: Comparison of peak signal to noise ratio

Image size (KB)	Peak signal to noise ratio (dB)		
	NTKFIBC-IS	Joint RCNN	LARKIFCM
21.3	54.15	52.56	50.06
15.4	52.56	50.06	49.04
16.5	54.15	51.22	48.13
19.8	56.08	54.15	52.56
23.2	52.56	50.06	49.04
26.9	51.22	50.28	48.13
20.4	50.06	48.13	47.30
17.9	51.22	49.04	48.13
25.1	52.56	50.06	49.04
24.6	54.15	52.56	50.06

The findings show that the NTKFIBC-IS methodology outperforms the other two techniques currently in use. For the sake of determining the peak signal-to-noise ratio, we will use the 21.3 KB picture. The NTKFIBC-IS approach has a mean square error of 0.25 and a peak signal to noise ratio of 54.15 dB. The mean square error and the peak signal to noise ratio are 0.36 and 52.56 dB, respectively, when using the Joint CNN [1]. Similarly, LARKIFCM [2] has a mean square error of 0.64 and a PSNR of 50.06 dB. The NTKFIBC-IS method has a lower mean square error and a greater peak signal-to-noise ratio, as shown by the statistics. As a consequence, 10 distinct outcomes may be found for each approach. There is a comparison of NTKFIBC-IS a finding with previously observed results. Averaging 10 findings, the NTKFIBC-IS approach improves the peak signal-to-noise ratio by 4% in comparison to [1] and 8% when compared to [2].

Fig. 2 shows the comparison of peak signal to noise ratio using three distinct methodologies. The following graph shows that the peak signal-to-noise ratio and the various retinal picture sizes as supplied in the horizontal direction may be examined on the vertical axis. The graph is non-linear because the input picture has varying degrees of noise. The two-dimensional graph shows that the suggested strategy improves performance outcomes when compared to the two previous approaches. For this enhancement, the Nonlinear Teager-Kaiser filtering method is used to eliminate noise artifacts from the original picture. Noiseless pixels are eliminated from the retinal picture in this procedure. This improves the image's quality while also reducing the mean square error.

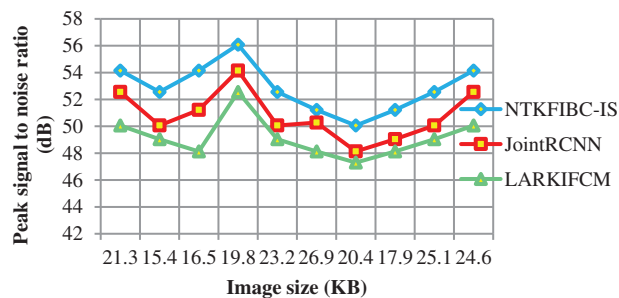


Figure 2: Graphical representation of the peak signal to noise ratio

Table 2 compares illness detection accuracy with the number of retinal pictures obtained from 10 to 100. Various methods provide different levels of precision. The obtained results show that the suggested NTKFIBC-IS method outperforms well in terms of obtaining greater accuracy. Ten retinal photos from the ARIMA database are here for consideration. For eight out of the ten photos, glaucoma or normal vision may be accurately identified at an average of 80 percent. The other two approaches [1,2] have an accuracy of 70% and 60%, respectively. The NTKFIBC-IS approach used in this statistical study delivers more accurate findings than the others. As with nine runs, different input picture counts are used for testing. In this comparison, the total observed NTKFIBC-IS findings are compared to the accuracy of the current results. When compared to conventional JointRCNN [1], LARKIFCM [2], the NTKFIBC-IS approach improves illness detection accuracy by 6% and 11%, respectively.

Table 2: Comparison of disease detection accuracy

Number of images	Disease detection accuracy (%)		
	NTKFIBC-IS	Joint RCNN	LARKIFCM
10	80	70	60
20	85	80	75
30	90	87	83
40	93	88	85
50	92	86	84
60	93	90	87
70	91	87	83
80	94	90	88
90	92	88	86
100	90	86	84

It is shown in Fig. 3 that the illness detection accuracy of 100 eye retinal pictures. As can be seen from the accompanying graphs, the accuracy varies depending on the number of input photographs. The suggested NTKFIBC-IS methodology has the best illness detection accuracy among the three techniques. Infomax Boost Clustering Based Segmentation and feature extraction are used to get these results. Image segmentation is done using a clustering approach known as an ensemble. The clinical characteristics are extracted from the image's area of interest, which is determined using the segmented findings. It is determined whether or not the picture contains evidence of glaucoma using the estimated feature value.

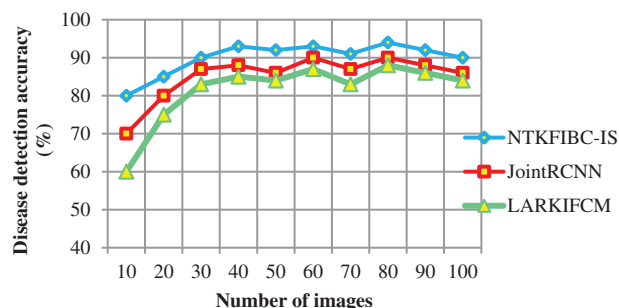


Figure 3: Graphical representation of the disease detection accuracy

Table 3 and Fig. 4 show the findings of illness detection time vs. the number of retinal pictures acquired from the ARIMA database. A shorter detection time may be achieved via preprocessing and segmentation, as shown by the observed outcomes. Detecting illness with accuracy takes longer because of the increased noise in the input photos. In addition; illness diagnosis is conducted using the whole picture, which takes longer to identify the supplied input image. Partitioning the input picture into parts solves this issue. For picture segmentation, the infomax boost clustering method is used. Glaucoma illness detection time is also reduced as a result of this.

Table 3: Comparison of disease detection time

Number of images	Disease detection time (ms)		
	NTKFIBC-IS	JointRCNN	LARKIFCM
10	17	20	23
20	24	26	30
30	27	30	33
40	32	35	38
50	38	40	43
60	40	44	48
70	44	47	49
80	48	52	56
90	52	55	58
100	55	57	60

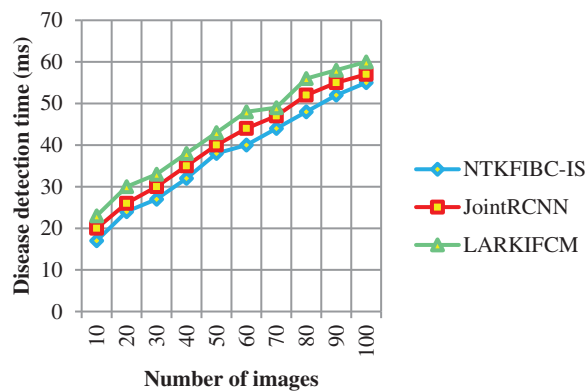


Figure 4: Graphical representation of the disease detection time

The illness detection time may be calculated using 10 retinal pictures in the first run. The illness detection times of [1] and [2] are 20 ms and 23 ms, respectively, but the NTKFIBC-IS approach takes 17 ms to complete. Additionally, each of the nine runs is conducted with a distinct number of retinal pictures. Results of the proposed NTKFIBC-IS methodology are compared to those of current techniques. A comparison of the NTKFIBC-IS approach with the two most recent techniques, JointRCNN [1] and LARKIFCM [2], shows an 8 percent and a 15 percent reduction in the time required to identify sickness.

4 Conclusion

The NTKFIBC-IS approach is obtained by automated screening systems to identify brain tumors, which is more accurate for early detection and tumor identification. To begin, the NTKFIBC-IS method uses nonlinear filtering to minimize the noise in the input MRI image and thus enhance image contrast. Once the preprocessed MRI image has been cleaned up, an ensemble clustering-based segmentation procedure is used to extract the most interesting parts of the area. Finally, the image's segmented portion is used to remove clinical characteristics that are next compared to a specified threshold value. As a consequence, photos of a normal brain tumor or a Brian tumor are appropriately identified. A picture database is used to undertake a complete experimental assessment. Analysis of the quantitative and qualitative performance of NTKFIBC-IS and other approaches is performed. The systematic quantitative findings confirmed to the NTKFIBC-IS methodology was implemented better than other relevant techniques in terms of improved illness diagnosis accuracy and shorter disease detection time.

Funding Statement: The authors received no specific funding for this study.

Conflicts of Interest: The authors declare that they have no conflicts of interest to report regarding the present study.

References

- [1] M. Soltaninejad, G. Yang, T. Lambrou, N. Allinson and T. L. Jones, "Supervised learning based multimodal mri brain tumor segmentation using texture features from supervoxels," *Computer Methods and Programs in Biomedicine*, vol. 157, pp. 64–89, 2018.
- [2] I. E. Kaya, A. C. Pehlivanlı, E. G. Sekizkardeş and T. Ibrikci, "Pca based clustering for brain tumor segmentation of t1w mri images," *Computer Methods and Programs in Biomedicine*, vol. 140, pp. 19–28, 2016.
- [3] A. P. Hagargi and D. C. Shubhangi, "Brain tumour detection and art classification technique in mr brain images using rpcaqt decomposition," *International Research Journal of Engineering and Technology (IRJET)*, vol. 5, no. 4, pp. 1–9, 2018.
- [4] C. R. Rao, M. N. V. S. S. Kumar and G. S. B. Rao, "A novel segmentation algorithm for feature extraction of brain MRI tumor," *Information and Decision Sciences*, vol. 701, pp. 455–463, 2018.
- [5] M. Latha and R. Surya, "Brain tumour detection using neural network classifier and k-means clustering algorithm for classification and segmentation," *International Journal of Computing Algorithm*, vol. 5, pp. 37–40, 2016.
- [6] N. Manasa, G. Mounica and B. D. Tejaswi, "Brain tumour detection based on canny edge detection algorithm and its area calculation," *Physics and Computer Science*, vol. 5, pp. 2347–8527, 2016.
- [7] R. Lavanyadevi, M. Machakowsalya, J. Nivethitha and A. N. Kumar, "Brain tumor classification and segmentation in mri images using pnn," in *2017 IEEE Int. Conf. on Electrical, Instrumentation, and Communication Engineering (ICEICE)*, Karur, India, pp. 1–6, 2017.
- [8] D. Desai and N. Chapatwala, "Brain extraction methods for magnetic resonance images (mri)," *International Journal of Innovative Research in Electrical, Electronics, Instrumentation and Control Engineering*, vol. 4, no. 5, pp. 1–6, 2016.
- [9] A. V. Prabu, A. Bharti, N. Guru and S. Tripathy, "Brain tumour detection in mri images using matlab," *International Journal of Scientific Research in Science, Engineering, and Technology*, vol. 2, no. 2, pp. 1230–1233, 2016.
- [10] D. N. George, H. B. Jehlol and A. S. A. Oleiwi, "Brain tumour detection using shape features and machine learning algorithms," *International Journal of Advanced Research in Computer Science and Software Engineering*, vol. 6, no. 12, pp. 454–459, 2015.
- [11] N. Boughattas, M. Berar, K. Hamrouni and S. Ruan, "Feature selection and classification using multiple kernel learning for brain tumor segmentation," in *2018 4th Int. Conf. on Advanced Technologies for Signal and Image Processing (ATSIP)*, Sousse, Tunisia, pp. 1–5, 2018.

- [12] S. T. Yassine, S. Sara, C. Bouchaib and R. Abdelilah, "A new fast brain tumor extraction method based on nl-means and expectation maximization," in *2018 4th Int. Conf. on Optimization and Applications (ICOA)*, Mohammedia, Morocco, pp. 1–5, 2018.
- [13] G. Jothi and H. H. Inbarani, "Hybrid tolerance rough set–firefly based supervised feature selection for mri brain tumor image classification," *Applied Soft Computing*, vol. 46, pp. 639–645, 2016.
- [14] S. Banerjee, S. Mitra and B. U. Shankar, "Automated 3d segmentation of brain tumors using visual saliency," *Information Sciences*, vol. 424, pp. 337–353, 2018.
- [15] A. Mukaram, C. Murthy and M. Z. Kurian, "An automatic brain tumour detection segmentation and classification using MRI image," *Computer Science and Technology*, vol. 6, no. 5, pp. 490–494, 2017.
- [16] G. B. Praveen and A. Agrawal, "Hybrid approach for brain tumor detection and classification in magnetic resonance images," in *2015 Communication, Control and Intelligent Systems (CCIS)*, vol. 9, pp. 162–166, 2015.
- [17] T. Rajesh, R. S. M. Malar and M. R. Geetha, "Brain tumor detection using optimization classification based on rough set theory," *Cluster Computing*, vol. 22, no. 1, pp. 1–7, 2019.
- [18] A. Arora, P. Roy, M. D. Shwetha, S. Venkatesan and R. Babu, "K-NN based classification of brain mri images using dwt and pca to detect different types of brain tumour," *International Journal of Medical Research & Health Sciences*, vol. 6, no. 9, pp. 15–20, 2017.
- [19] Praveen and A. Singh, "Detection of a brain tumor in mri images using a combination of fuzzy c-means and svm," in *2015 2nd Int. Conf. on Signal Processing and Integrated Networks (SPIN)*, Noida, India, 2015.
- [20] A. Chinnu, "Mri brain tumor classification using svm and histogram-based image segmentation," *Chinnu A/ (IJCSIT) International Journal of Computer Science and Information Technologies*, vol. 6, no. 2, pp. 1505–1508, 2015.
- [21] S. K. Saha, "Modeling statistical dopant fluctuations effect on threshold voltage of scaled JFET devices," *IEEE Access*, vol. 4, pp. 507–513, 2016.
- [22] P. Juneja, S. Kaur, H. Sharma and P. Kumar, "Comparative analysis of various medical image segmentation methodologies in temporal order," *Journal of Natural Remedie*, vol. 21, no. 2, pp. 170–177, 2020.